


Non-obstructive high-risk plaques increase the risk of future culprit lesions comparable to obstructive plaques without high-risk features: the ICONIC study

Richard A. Ferraro¹, Alexander R. van Rosendael^{1,2}, Yao Lu³, Daniele Andreini⁴, Mouaz H. Al-Mallah⁵, Filippo Cademartiri⁶, Kavitha Chinnaiyan⁷, Benjamin J.W. Chow⁸, Edoardo Conte⁴, Ricardo C. Cury⁹, Gudrun Feuchtner¹⁰, Pedro de Araújo Gonçalves¹¹, Martin Hadamitzky¹², Yong-Jin Kim¹³, Jonathon Leipsic¹⁴, Erica Maffei¹⁵, Hugo Marques¹¹, Fabian Plank¹⁶, Gianluca Pontone⁴, Gilbert L. Raff⁷, Todd C. Villines¹⁷, Sang-Eun Lee¹⁸, Subhi J. Al'Aref¹, Lohendran Baskaran^{1,19}, Iksung Cho^{18,20}, Ibrahim Danad²¹, Heidi Gransar²², Matthew J. Budoff²³, Habib Samady²⁴, Peter H. Stone²⁵, Renu Virmani²⁶, Jagat Narula²⁷, Daniel S. Berman²⁸, Hyuk-Jae Chang¹⁸, Jeroen J. Bax², James K. Min¹, Leslee J. Shaw¹, and Fay Y. Lin ^{1*}

¹Department of Radiology, New York-Presbyterian Hospital, Weill Cornell Medicine, 413 E 69th Street, Suite 108, New York, NY 10021, USA; ²Department of Cardiology, Leiden University Medical Center, Cardiology, Albinusdreef 2, Leiden, Zuid-Holland 2333 ZA, The Netherlands; ³Department of Healthcare Policy and Research, New York-Presbyterian Hospital, Weill Cornell Medical College, 413 E 69th Street, Suite 108, New York, NY 10021, USA; ⁴Centro Cardiologico Monzino, IRCCS, Via Carlo Parea, 4, 20138 Milano MI, Italy; ⁵Houston Methodist DeBakey Heart & Vascular Center, Houston Methodist Hospital, 6565 Fannin Street, Houston, TX 77030, USA; ⁶Cardiovascular Imaging Center, SDN IRCCS, via Gianturco 113, 80143 Naples, Italy; ⁷Department of Cardiology, William Beaumont Hospital, 3601 W 13 Mile Rd, Royal Oak, MI 48073, USA; ⁸Department of Medicine and Radiology, University of Ottawa, 451 Smyth Rd #2044, Ottawa, ON K1H 8M5, Canada; ⁹Department of Radiology, Miami Cardiac and Vascular Institute, 8900 N Kendall Dr., Miami, FL 33176, USA; ¹⁰Department of Radiology, Medical University of Innsbruck, Innsbruck, Austria; ¹¹UNICA, Unit of Cardiovascular Imaging, Hospital da Luz, Av. Lusíada 100, 1500-650 Lisbon, Portugal; ¹²Department of Radiology and Nuclear Medicine, German Heart Center Munich, Lazarettstraße 36, 80636 Munich, Germany; ¹³Division of Cardiology, Department of Internal Medicine, Seoul National University College of Medicine, Seoul National University Hospital, 101 Daehak-ro, Jongno-gu, Seoul, Seoul 110-744, Republic of South Korea; ¹⁴Department of Medicine and Radiology, University of British Columbia, 2775 Laurel St. Vancouver, BC V5Z 1M9 Canada; ¹⁵Department of Radiology, Area Vasta 1/ASUR Marche, Viale Federico Comandino, 70, 61029 Urbino, Italy; ¹⁶Department of Cardiology, Innsbruck Medical University, Christoph-Probst-Platz 1, Innrain 52 A, 6020 Innsbruck, Austria; ¹⁷Department of Medicine, University of Virginia Health System, 1215 Lee St, Charlottesville, VA 22908, USA; ¹⁸Severance Cardiovascular Hospital and Severance Biomedical Science Institute, Division of Cardiology, Yonsei University College of Medicine, Yonsei University Health System, 50-1 Yonsei-ro, Seodaemun-gu, Seoul, Seoul 120-752, Republic of South Korea; ¹⁹National Heart Centre, 5 Hospital Dr, Singapore 169609, Singapore; ²⁰Chung-Ang University Hospital, Dongjak-gu, Heukseok-dong, Heukseok-ro, Seoul, 102 KR 06973, Republic of South Korea; ²¹Department of Cardiology, Amsterdam University Medical Center, VU University Medical Center, De Boelelaan 1117, 1081 HV, 1VU University Medical Center, Amsterdam, The Netherlands; ²²Department of Imaging, Cedars Sinai Medical Center, 8700 Beverly Blvd, Taper 1258, Los Angeles, CA 90048, USA; ²³Department of Medicine, Los Angeles Biomedical Research Institute, 1124 W Carson St, Torrance, CA 90502, USA; ²⁴Division of Cardiology, Department of Medicine, Emory University School of Medicine, 100 Woodruff Circle, Atlanta, GA 30322, USA; ²⁵Department of Cardiovascular Medicine, Brigham and Women's Hospital, 75 Francis St, Boston, MA 02115, USA; ²⁶Department of Pathology, CVPath Institute, 19 Firstfield Rd, Gaithersburg, MD 20878, USA; ²⁷Division of Cardiology, Department of Medicine, Icahn School of Medicine at Mount Sinai, Mount Sinai Heart, Zena and Michael A. Wiener Cardiovascular Institute, and Marie-Josée and Henry R. Kravis Center for Cardiovascular Health, One Gustave L Levy Place, Box 1030, New York, NY 10029, USA; and ²⁸Department of Imaging and Medicine, Cedars Sinai Medical Center, 8705 Gracie Allen Dr, Los Angeles, CA 90048, USA

Received 20 September 2019; editorial decision 28 February 2020; accepted 6 March 2020; online publish-ahead-of-print 13 June 2020

Aims

High-risk plaque (HRP) and non-obstructive coronary artery disease independently predict adverse events, but their importance to future culprit lesions has not been resolved. We sought to determine in patients prior to confirmed acute coronary syndrome (ACS) the association between lesion percent diameter stenosis (%DS), and the absolute number and prevalence of HRP. The secondary objective was to examine the relative importance of non-obstructive HRP in future culprit lesions.

Methods and results

Within the ICONIC study, a nested case–control study of patients undergoing coronary computed tomographic angiography (coronary CT), we included ACS cases with culprit lesions confirmed by invasive coronary angiography and coregistered to baseline coronary CT. Quantitative CT was used to evaluate obstructive ($\geq 50\%$) and non-obstructive ($< 50\%$) diameter stenosis, with HRP defined as ≥ 2 features of spotty calcification, positive remodelling, or low-attenuation plaque at baseline. A total of 234 patients with downstream ACS over 54 (interquartile range 5–525.5) days exhibited 198/898 plaques with HRP on coronary CT. While HRP was less prevalent in non-obstructive (19.7%, 161/819) than obstructive lesions (46.8%, 37/79, $P < 0.001$), non-obstructive plaque comprised 81.3% (161/198) of HRP lesions overall. Among the 128 patients with identifiable culprit lesion precursors, the adjusted hazard ratio (HR) was 1.85 [95% confidence interval (CI) 1.26–2.72] for HRP, with no interaction between %DS and HRP ($P = 0.82$). Compared to non-obstructive HRP lesions, obstructive lesions without HRP exhibited a non-significant HR of 1.41 (95% CI 0.61–3.25, $P = 0.42$).

Conclusions

While HRP is more prevalent among obstructive lesions, non-obstructive HRP lesions outnumber those that are obstructive and confer risk clinically approaching that of obstructive lesions without HRP.

Keywords

Coronary computed tomographic angiography • coronary artery disease • myocardial infarction

Introduction

Although obstructive coronary artery disease (CAD) evaluation forms the basis of risk stratification in cardiac disease, the majority of myocardial infarction (MI) precursors are derived from non-obstructive plaque.^{1–6} High-risk plaque (HRP) evaluation via coronary computed tomographic angiography (coronary CT) has been demonstrated to predict patients at high risk for coronary events.^{7–9} Recent substudies of the PROMISE trial have highlighted the prognostic value of non-obstructive CAD and HRP in the coronary CT arm.^{5,10} However, the association of HRP and atherosclerotic plaque characteristics (APCs) in patients with downstream acute coronary syndrome (ACS), and for culprit lesions responsible for ACS, remains unclear.^{10–13}

The aim of this study was to determine in patients prior to confirmed ACS the association between the degree of CAD as evaluated by baseline coronary CT, and the absolute number and prevalence of HRP. We also examined the relative importance of HRP for the outcome of becoming a culprit lesion in obstructive vs. non-obstructive CAD.

Methods

Patient population and study design

The ICONIC study, a nested case–control study within the CONFIRM registry of 25 416 consecutive patients undergoing baseline coronary CT, was comprised of 234 adjudicated patients with subsequent ACS events and propensity-matched non-event controls.² As previously described, patients were excluded for prior CAD, death without antecedent ACS, insufficient data for adjudication, and interval elective revascularization of a culprit segment.² Only ACS cases (40 ST-elevation MI, 114 non-ST-elevation MI, 6 MI that could not be distinguished, and 74 unstable angina) were included in the current study. The study endpoint was ACS as defined by WHO/MONICA universal definition of MI.^{14,15} Adjudication of ACS events was performed at a centralized data coordinating centre blinded from coronary CT data and utilizing the definition of ACS, as above.²

For culprit lesion subanalysis, masked adjudication of culprits by invasive coronary angiography (ICA) was performed using the ROMICAT

convention of one culprit per patient and subsequently aligned to lesions on baseline coronary CT.² A total of 162 culprit lesions were identified via ICA, of which 129 could be coregistered to baseline coronary CT (5 had no baseline CAD visible by coronary CT, 12 had baseline lesions unmeasurable due to artefact or spatial resolution, and 17 had lesions by coronary CT elsewhere but none that could be aligned to the ICA-identified lesion). Five of the culprit lesions were total occlusions that were not analysed for plaque volume or plaque characteristics, of whom four had non-culprit lesions elsewhere that were included. In total, 128 patients with 124 culprit lesions were included for subanalysis.

Imaging procedure and lesion analysis

All coronary CT evaluations were conducted using single-source and dual-source ≥ 64 -detector rows scanners (vendors varying by institution), and imaging data obtained via prospective axial triggering or retrospective helical electrocardiogram-gating.² Coronary CT measurements were evaluated by a blinded core lab using semi-automated plaque analysis software (MEDIS QAngio CT Research Edition v2.1.9.1, Medis Medical Imaging Systems, Leiden, Netherlands).^{2,16}

A lesion with atherosclerosis was defined as any tissue $> 1 \text{ mm}^2$ within or adjacent to the lumen that can be discriminated from surrounding pericardial tissue, epicardial fat, or lumen, and identified in > 2 planes. Obstructive lesions were defined as $\geq 50\%$ DS, and non-obstructive lesions were $< 50\%$ DS.^{17,18} Quantitative CT measurements included plaque volume, length, cross-sectional plaque burden, minimal lumen diameter, minimal lumen area, and plaque volume by composition: calcified [Hounsfield Unit (HU) > 350], non-calcified (HU ≤ 350), and fibrofatty and necrotic core (HU ≤ 130). Remodelling index was calculated using comparisons of mean vessel area within 5 mm proximal and distal to the lesion.²

Lesions were additionally evaluated for qualitative APCs: positive remodelling (PR) defined as a remodelling index ≥ 1.1 , spotty calcification (SC) defined by visualized observed calcification $\leq 3.3 \text{ mm}$ in any direction within a plaque, and low-attenuation plaque (LAP) defined as $< 30 \text{ HU}$. Using these characteristics, HRP lesions were defined as the presence of two or more of the above APCs within any one plaque (Figure 1).² Napkin-ring sign, defined as a circumferential area of a non-calcified plaque that displays greater attenuation than the central portion with LAP, was also assessed as an APC, though not included in the definition of HRP due to low prevalence.^{2,19} Vessel location and distance to the ostium were also recorded.

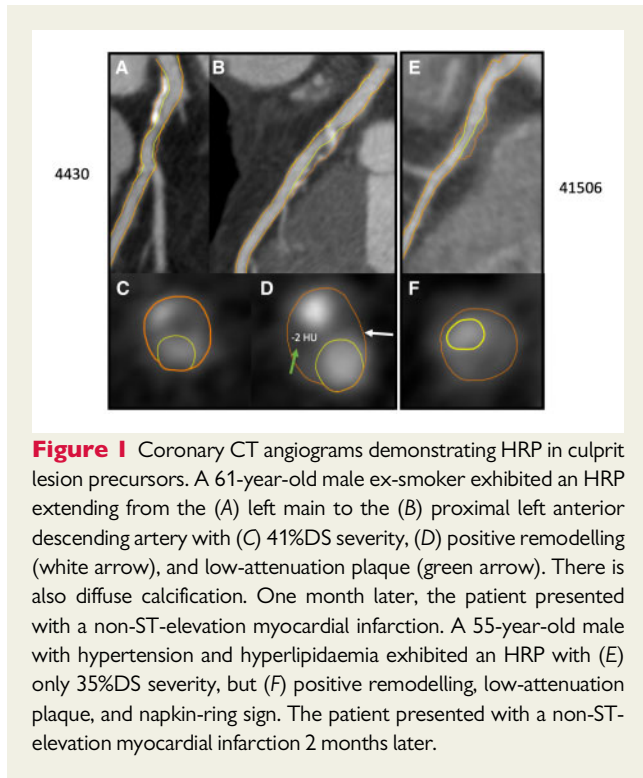


Figure 1 Coronary CT angiograms demonstrating HRP in culprit lesion precursors. A 61-year-old male ex-smoker exhibited an HRP extending from the (A) left main to the (B) proximal left anterior descending artery with (C) 41%DS severity, (D) positive remodelling (white arrow), and low-attenuation plaque (green arrow). There is also diffuse calcification. One month later, the patient presented with a non-ST-elevation myocardial infarction. A 55-year-old male with hypertension and hyperlipidaemia exhibited an HRP with (E) only 35%DS severity, but (F) positive remodelling, low-attenuation plaque, and napkin-ring sign. The patient presented with a non-ST-elevation myocardial infarction 2 months later.

Per-patient level maximal percent diameter stenosis (%DS) was summarized as the maximum quantitative CT %DS among all lesions, with total occlusions assigned as 100%, and classified into six subgroups (0%, 1–24%, 25–49%, 50–69%, 70–99%, and 100%). For culprit lesion subanalysis, patients were classified into four subgroups: non-obstructive HRP negative, non-obstructive HRP positive, obstructive HRP negative, and obstructive HRP positive.

Primary and secondary outcomes

The primary outcome was HRP number and prevalence. The secondary outcome was the odds of becoming a culprit lesion.

Statistical analysis

Continuous variables were reported as median \pm interquartile range (IQR) and categorical variables as counts with percentage. Trends for continuous variables between %DS subgroups were assessed using the Pearson's correlation coefficient and trends for categorical variables were assessed using the Cochran Armitage test or χ^2 test if Cochran Armitage test was not applicable. For the secondary outcome of becoming a culprit lesion, marginal Cox proportional hazard model adjusted for patient effects was performed to assess the predictive value of HRP, %DS, and its interaction. Multivariable models were constructed with adjustment for cardiac risk factors, angina typicality, and body mass index. For interactions, stenosis severity was dichotomized at the 50% threshold for obstructive lesions. A sensitivity analysis was performed restricted to MI outcomes only. Two-sided *P*-values of <0.05 were considered statistically significant. All statistical analyses were conducted using R (Version 3.3.0, R Development Core Team, 2016) and SAS (Version 9.4, SAS Institute Inc., Cary, NC, USA) software packages.

Results

Patient characteristics

A total of 234 patients (age 62.2 ± 11 years, 63% male) with ACS were included in this study. Median time to ACS was 54 (IQR 5–525.5) days. The most common baseline %DS subgroup in patients prior to ACS was 25–49% (43% of patients). There was no significant association among cases between maximal %DS and underlying risk factors, chest pain typicality, or type of ACS (Table 1).

Association of HRP and APCs with %DS on baseline coronary CT

A total of 898 baseline lesions were observed in 234 patients. The number of lesions was highest for lower %DS, and the majority (819/898, 91.2%) were non-obstructive (Figure 2A and Table 2). HRP was observed in 198/898 (22%) of baseline lesions in patients. PR was the most common APC overall (699/898, 77.8%), with a lower prevalence of SC (119/898, 13.3%), and LAP (155/898, 17.2%). The absolute number of APCs was significantly greater in non-obstructive lesions, comprising 639/699 (91.4%) of all lesions with PR, 125/155 (80.6%) with LAP, and 97/119 (81.5%) of all lesions with SC. All APCs were significantly more prevalent with increasing %DS ($P < 0.0001$) (Table 2).

The absolute number of HRP positive lesions was higher with lower %DS, with non-obstructive lesions comprising 161/198 (81.4%) of all lesions with HRP (Figure 2B). Similar to the trend for APCs, the prevalence of HRP was significantly lower in non-obstructive (161/819, 19.7%) than in obstructive (37/79, 46.8%) lesions (test for trend $P < 0.001$, Figure 2C).

Culprit lesion subset

A total of 128 patients with 124 confirmed culprit lesion precursors exhibited 595 baseline lesions, with 4 culprit lesions excluded as total occlusions could not be evaluated by quantitative coronary CT. Ninety-seven of 124 (78.2%) culprit lesions were non-obstructive, and 40 of 124 (32.3%) exhibited HRP. The risk of becoming a culprit lesion increased with greater %DS. Compared to %DS of 1–24%, the hazard ratio (HR) of becoming a culprit for 25–49%DS was 2.49 [95% confidence interval (CI) 1.66–3.74] and for 50–69%DS lesions was 4.40 (95% CI 2.33–8.34, Table 3). With only four lesions in the 70–99% subgroup, no significant increase in becoming a culprit could be observed (HR 1.10, 95% CI 0.15–8.20). HRP also increased the risk of becoming a culprit lesion (HR 1.85, 95% CI 1.26–2.72). There was no significant interaction between $\geq 50\%$ DS and HRP ($P = 0.82$). Both %DS and HRP (adjusted HR 1.78, 95% CI 1.21–2.62) remained significant predictors after multivariable adjustment. HRs were similar when restricted to 82 patients with MI (HRP adjusted HR 1.96, 95% CI 1.19–3.21, Supplementary data online).

Categorically, as compared to non-obstructive HRP negative lesions, non-obstructive HRP positive lesions (HR 1.67, 95% CI 1.07–2.60) and obstructive but HRP negative lesions (HR 2.35, 95% CI 1.10–5.03) exhibited increasingly elevated risks of becoming a culprit lesion, with a non-significant difference between the two categories (HR 1.41, 95% CI 0.61–3.25, $P = 0.42$, Figure 3). After multivariable adjustment, a similar trend was observed (non-obstructive HRP positive adjusted HR 1.42, 95% CI 0.90–2.26, $P = 0.13$; obstructive HRP

Table 1 Characteristics of ACS patients by baseline maximally stenotic segment

| Maximum % diameter stenosis | All (n = 234) | 0% (n = 15) | 1–24% (n = 37) | 25–49% (n = 101) | 50–69% (n = 51) | 70–99% (n = 6) | 100% (n = 24) | P-test for trend |
|--|---------------|------------------|------------------|------------------|-----------------|----------------|------------------|------------------|
| Age (years), median (IQR) | 63 (55–76) | 63 (49–69) | 60 (52–68) | 64 (54–69) | 68 (58–74) | 59.5 (47–61) | 63 (55–71) | 0.10 |
| Male gender, N (%) | 85 (36) | 6 (40) | 29 (78) | 63 (62) | 31 (61) | 5 (83) | 15 (63) | 0.85 |
| BMI (kg/m ²), median (IQR) | 26.5 (24–30) | 26.4 (23.4–31.6) | 27.6 (24.9–30.7) | 26 (24.0–29.5) | 26.8 (23.8–30) | 29 (27.7–30.5) | 26.1 (24.1–29.2) | 0.27 |
| Risk factors, N (%) | | | | | | | | |
| Hypertension | 148 (63) | 9 (60) | 21 (57) | 63 (62) | 34 (67) | 4 (67) | 17 (71) | 0.17 |
| Hyperlipidaemia | 129 (55) | 8 (53) | 19 (51) | 56 (55) | 28 (55) | 5 (83) | 13 (54) | 0.62 |
| Diabetes | 46 (20) | 3 (20) | 1 (3) | 26 (26) | 11 (22) | 1 (17) | 4 (17) | 0.54 |
| Smoking current | 72 (31) | 5 (33) | 12 (32) | 27 (27) | 16 (31) | 3 (50) | 9 (38) | 0.50 |
| Smoking past | 79 (34) | 2 (13) | 14 (38) | 32 (32) | 19 (37) | 4 (67) | 8 (33) | 0.26 |
| Family history | 94 (40) | 8 (53) | 14 (38) | 45 (45) | 13 (25) | 5 (83) | 9 (38) | 0.49 |
| Race/ethnicity, N (%) | | | | | | | | |
| White | 112 (48) | 7 (47) | 19 (51) | 48 (48) | 26 (51) | 3 (50) | 9 (38) | 0.38 |
| East Asian | 53 (23) | 3 (20) | 3 (8) | 25 (25) | 13 (25) | 1 (17) | 8 (33) | 0.06 |
| Others/unknown | 69 (29) | 5 (33) | 15 (41) | 28 (28) | 12 (24) | 2 (33) | 7 (29) | 0.60 |
| Symptoms, N (%) | | | | | | | | |
| Syncope, dyspnea or palpitations | 37 (16) | 1 (7) | 14 (38) | 12 (12) | 6 (12) | 1 (17) | 3 (13) | 0.18 |
| Non-cardiac CP | 28 (12) | 4 (27) | 5 (14) | 11 (11) | 7 (14) | 0 (0) | 1 (4) | 0.08 |
| Atypical CP | 94 (40) | 6 (40) | 9 (24) | 46 (46) | 19 (37) | 2 (33) | 12 (50) | 0.18 |
| Typical CP | 63 (27) | 3 (20) | 8 (22) | 26 (26) | 18 (35) | 3 (50) | 5 (21) | 0.35 |
| Typicality unknown | 12 (5) | 1 (7) | 6 (16) | 15 (15) | 7 (14) | 1 (17) | 2 (8) | 0.41 |
| Dyspnoea | 40 (17) | 1 (7) | 8 (22) | 16 (16) | 9 (18) | 1 (17) | 5 (21) | 0.72 |
| ACS type, N (%) | | | | | | | | |
| STEMI | 40 (17) | 2 (13) | 10 (27) | 15 (15) | 6 (12) | 2 (33) | 5 (21) | 0.93 |
| NSTEMI/MI NOS | 120 (52) | 10 (67) | 19 (51) | 50 (50) | 23 (45) | 3 (50) | 15 (63) | 0.99 |
| UA | 74 (32) | 3 (20) | 8 (22) | 36 (36) | 22 (43) | 1 (17) | 4 (17) | 0.96 |

ACS, acute coronary syndrome; BMI, body mass index; CP, chest pain; MI NOS, myocardial infarction not otherwise specified; NSTEMI, non-ST-elevation myocardial infarction; STEMI, ST-elevation myocardial infarction; UA, unstable angina.

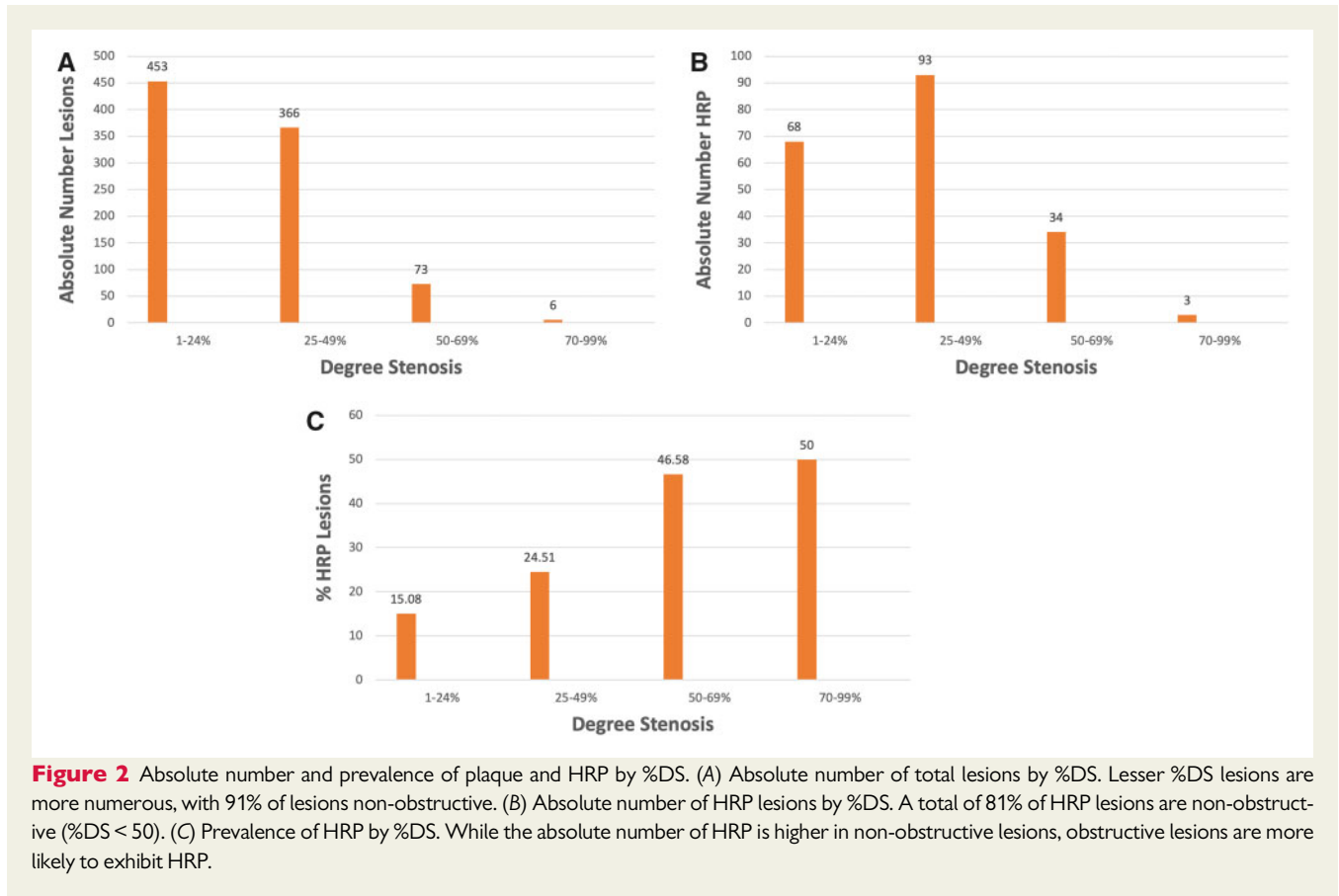
negative adjusted HR 2.33, 95% CI 1.1–5.03, $P=0.21$), with a non-significant increase over the two categories in risk (adjusted HR 1.68, 95% CI 0.75–3.75, $P=0.20$) and positive predictive value [26/109 (24%) vs. 13/34 (38%), $P=0.10$]. Restricted to MI, the risk of non-obstructive HRP positive lesions (adjusted HR 1.97, 95% CI 1.10–3.52, $P=0.02$) and obstructive but HRP negative lesions (adjusted HR 2.38, 95% CI 0.99–5.69, $P=0.05$) was also elevated to a comparable degree (adjusted HR 1.21, 95% CI 0.45–3.22, $P=0.70$).

Discussion

In this large multicentre cohort of patients with baseline coronary CT and subsequent ACS, we observed that non-obstructive HRP positive lesions outnumber obstructive HRP positive lesions and increase the risk of becoming a culprit to a level approaching that of obstructive HRP negative lesions. A total of 81.4% of all HRP lesions are non-obstructive, despite the increased prevalence of HRP with higher %DS. Among patients with future ACS, HRP at baseline independently increases the risk of becoming a culprit in both obstructive and non-obstructive CAD (HR 1.85, 95% CI 1.26–2.72), without significant interaction with %DS ($P=0.82$).

Our results are consistent with an underappreciated aspect of the HRP substudies of the PROMISE and SCOT-HEART trials, wherein non-obstructive HRP positive lesions conferred risk comparable to that of obstructive HRP negative lesions. In PROMISE, the HR for non-obstructive HRP positive patients was 4.31 (95% CI 2.25–8.26) compared to patients with no plaque, overlapping with the CI for obstructive HRP negative patients of 9.31 (95% CI 4.21–20.61); in SCOT-HEART, a similar overlap was observed of HR 5.81 (95% CI 1.50–22.46) compared to HR 7.73 (95% CI 1.73–34.54).^{10,20} In addition, we observed consistent effects both for ACS and the subset of patients with MI.

Our study differs from the PROMISE and SCOT-HEART studies in performing a lesion level, not patient level, analysis of precursors of ICA-identified culprit lesions in a cohort of patients with ACS; because of the design, and the lower obstructive CAD threshold of $\geq 50\%$ DS, we observe smaller HRs with a largely consistent trend in findings. The case–control design of the ICONIC study leads to additional important differences from the SCOT-HEART and PROMISE studies. SCOT-HEART observed an independent predictive value of HRP above stenosis severity alone, but not above coronary calcium as a proxy of aggregate plaque burden. However, the parent ICONIC study, by matching ACS cases with controls propensity



matched for CAD risk factors and stenosis severity, observed that in cases and controls with comparable plaque burden, HRP was significantly elevated in cases.² Furthermore, histologic evidence suggests that coronary calcium predicts risk on a per patient, but not per-lesion level.²¹ In the PROMISE trial, HRP significantly elevated risk in the stratum of non-obstructive patients, but not in obstructive patients. There may have been too few obstructive patients with %DS $\geq 70\%$ to observe a significant difference in the low-risk PROMISE cohort. In our study of ACS patients, interaction testing to formally evaluate effect modification demonstrated no difference in the per-lesion risk of HRP by strata of %DS.¹⁰ Invasive imaging trials, such as PROSPECT, also did not evaluate interactions between HRP and %DS.²² Our data thus lend support to reporting HRP even among non-obstructive lesions, as recommended by the CADRADS guideline.²³

The abundance of non-obstructive HRP negative lesions in patients with future ACS, despite the higher likelihood of HRP in obstructive lesions, has been observed by invasive imaging and coronary CT.^{10,11} Tian *et al.*¹¹ utilized invasive imaging in patients undergoing ICA for both stable CAD and ACS and found the absolute number of thin cap fibroatheromas was three times greater in <70% stenoses as compared to $\geq 70\%$. Using coronary CT, which permits the evaluation of mild (<30%) stenoses not well evaluated by invasive imaging, we observe more than four times the absolute number of HRP in non-obstructive as compared to obstructive lesions prior to ACS,

and more than 60 times the number of HRP in non-severe as compared to severe stenosis. We believe this aligns with findings calculated from the PROMISE trial, wherein the abundance of non-obstructive HRP positive patients resulted in a large attributable fraction of major adverse cardiac events (18.3%), higher than the attributable fraction of obstructive HRP positive (14.5%) and obstructive HRP negative (8.4%) patients.¹⁰

We also observed that the prevalence of HRP increased with increasing %DS, similar to prior invasive and coronary CT studies.^{10,11} Thus, in clinical practice, while obstructive HRP positive lesions are infrequent, salient, and thus attractive candidates for invasive intervention, non-obstructive HRP positive lesions represent a greater denominator of underappreciated risk for treatment on a per-patient level. In modelling studies, improved medical management in both obstructive and non-obstructive CAD may partially account for the long-term benefit of the coronary CT arm in the SCOT-HEART trial.^{13,24} Our study lends support for shared decision-making on intensity of medication management in non-obstructive CAD, particularly if HRP positive. While only a quarter of HRP positive non-obstructive lesions will become culprits in future ACS patients, it remains a source of elevated risk. Future analyses should evaluate the role of HRP positive and HRP negative non-obstructive lesions in optimal medical management, and the generalizability of our results to non-obstructive HRP diagnosed by invasive coronary imaging.

Table 2 Individual lesion CT characteristics by baseline diameter stenosis

| %DS | Total (n = 898) | 1–24% (n = 453) | 25–49% (n = 366) | 50–69% (n = 73) | 70–99% (n = 6) | P-value |
|---|------------------|------------------|-------------------|--------------------|--------------------|---------|
| Stenosis measures, median (IQR) | | | | | | |
| Minimal lumen area (mm ²) | 3.2 (2.1–5.0) | 4.4 (2.9–6.9) | 2.6 (1.8–3.9) | 1.6 (1.1–2.1) | 0.3 (0.1–0.9) | <0.0001 |
| %DS (continuous) | 24.9 (14.6–37.2) | 14.6 (8.1–19.4) | 34.5 (29.1–41.2) | 56.2 (52.4–63.2) | 74.9 (71.9–75.5) | <0.0001 |
| Lesion location | | | | | | |
| LM, N (%) | 29 (3) | 16 (4) | 12 (3) | 1 (1) | 0 (0) | 0.38 |
| LAD, N (%) | 365 (41) | 158 (35) | 170 (46) | 35 (48) | 2 (33) | 0.002 |
| LCx, N (%) | 203 (23) | 114 (25) | 75 (20) | 12 (16) | 2 (33) | 0.08 |
| RCA, N (%) | 301 (34) | 165 (36) | 109 (30) | 25 (34) | 2 (33) | 0.18 |
| Distance to ostium (mm), median (IQR) | 37.8 (23.5–59.1) | 38.1 (23.0–62.3) | 37.7 (23.9–55.2) | 37.8 (27.0–54.5) | 26.5 (23.7–33.7) | 0.77 |
| Quantitative computed tomography measurements, median (IQR) | | | | | | |
| Plaque volume (mm ³) | 29.8 (11.7–90.8) | 18.0 (7.9–38.9) | 50.2 (17.9–125.8) | 150.2 (75.4–303.3) | 146.9 (96.9–186.9) | <0.0001 |
| Calcified plaque (mm ³) | 6.4 (1.3–23.4) | 3.6 (0.8–10.5) | 11.1 (2.4–34.2) | 44.4 (9.1–94.3) | 81.1 (22.7–109.1) | <0.0001 |
| Non-calcified plaque (mm ³) | 19.5 (6.1–56.1) | 12.3 (4.5–28.9) | 32.7 (8.4–80.2) | 89.9 (40.2–197.9) | 74.3 (37.8–105.9) | <0.0001 |
| Fibrofatty/necrotic core (mm ³) | 2.8 (0.2–14.4) | 1.2 (0.1–6.1) | 4.8 (0.4–23.4) | 17.7 (5.4–64.3) | 7.97 (7.69–10.12) | <0.0001 |
| Remodelling index | 1.3 (1.1–1.6) | 1.3 (1.2–1.6) | 1.3 (1.1–1.6) | 1.3 (1.1–1.6) | 1.2 (1.1–1.5) | 0.69 |
| Lesion length (mm) | 19.4 (13.8–32.2) | 16.1 (12.7–22.3) | 24.0 (16.0–38.5) | 43.1 (28.6–61.2) | 36.7 (33.5–62.0) | <0.0001 |
| Atherosclerotic plaque characteristics, N (%) | | | | | | |
| PR | 699 (78) | 376 (83) | 263 (72) | 55 (75) | 5 (83) | 0.003 |
| SC | 119 (13) | 44 (10) | 53 (14) | 20 (27) | 2 (33) | <0.0001 |
| LAP | 155 (17) | 46 (10) | 79 (22) | 29 (40) | 1 (17) | <0.0001 |
| NRS | 14 (2) | 4 (1) | 6 (2) | 3 (4) | 1 (17) | 0.007 |
| HRP | 198 (22) | 68 (15) | 93 (25) | 34 (47) | 3 (50) | <0.0001 |

%DS, percent diameter stenosis; HRP, high-risk plaque; LAD, left anterior descending artery; LAP, low-attenuation plaque; LCx, left circumflex artery; LM, left main artery; NRS, napkin-ring sign; PR, positive remodelling; RCA, right coronary artery; SC, spotty calcification.

Table 3 HR of becoming a culprit lesion by stenosis severity and HRP

| Percent diameter stenosis | Unadjusted HR | P-value | Adjusted HR ^a | P-value |
|-------------------------------|------------------|---------|--------------------------|---------|
| 1–24% | 1 | | 1 | |
| 25–49% | 2.49 (1.66–3.74) | <0.0001 | 2.34 (1.52–3.61) | 0.0001 |
| 50–69% | 4.40 (2.33–8.34) | <0.0001 | 5.23 (2.81–9.72) | <0.0001 |
| 70–99% ^b | 1.10 (0.15–8.20) | 0.925 | 1.28 (0.16–10.21) | 0.81 |
| HRP | 1.85 (1.26–2.72) | 0.001 | 1.78 (1.21–2.62) | 0.003 |
| Interaction HRP and DS (≥50%) | 0.89 (0.31–2.50) | 0.82 | 1.31 (0.49–3.46) | 0.59 |

BMI, body mass index; DS, degree stenosis; HR, hazard ratio; HRP, high-risk plaque.

^aAdjusted for CAD risk factors, BMI, and angina typicality.

^bOnly four baseline lesions in the subset were between 70% and 99%.

Study limitations

HRP is well validated for elevated risk, but its utility in risk assessment and therapy has not been defined.^{10–12,22,25} The ICONIC study is unique in specifically examining the impact of baseline HRP on later culprit lesions identified by ICA at the time of first ACS, but cannot estimate diagnostic performance or generate risk scores given its case–control design. There may be information and referral bias inherent to the design of ICONIC as a retrospective nested case–control study. With a larger sample size, the HR of non-obstructive HRP positive lesions and obstructive HRP

negative lesions may have reached statistical significance; nevertheless, the magnitude of risk is still clinically comparable and is consistent with substudies for PROMISE and SCOT-HEART.^{10,20} We could not evaluate dynamic changes in HRP that may have occurred between baseline coronary CT and ACS, which may further elucidate the contribution of HRP to later events, and may be better addressed by serial coronary CT studies.²⁶ The risks of non-obstructive HRP positive lesions may have been biased because total occlusions were not evaluated for HRP, and because patients with ACS caused by elective revascularization between

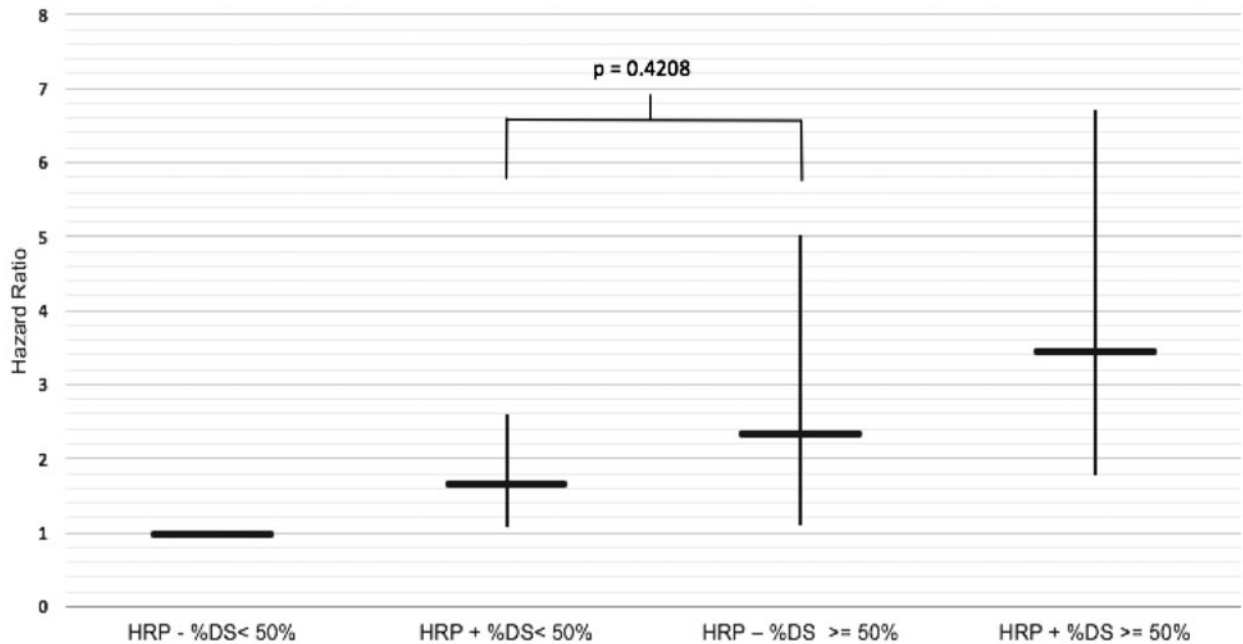


Figure 3 Hazard ratio of becoming a culprit lesion by combinations of the presence of HRP and obstructive CAD. The presence of HRP elevates the risk of non-obstructive lesions to a level that nears that of an HRP–obstructive lesion ($P = 0.42$). There is no significant interaction between HRP and obstructive %DS ($P = 0.91$).

the coronary CT and ACS were excluded. However, among the seven excluded patients with elective percutaneous coronary intervention and later ACS due to stent restenosis or thrombosis, only one exhibited HRP in the baseline lesion prior to the elective revascularization, supporting the histologic observation that stable obstructive CAD tends to exhibit less vulnerable plaque. Finally, due to the case–control design of ICONIC, our substudy results cannot be generalized to primary prevention, and the risk of non-obstructive HRP in primary prevention may differ from what we observe. Furthermore, lesions with only one APC fall below the threshold of classification of HRP and may represent a large denominator of risk. Future studies should derive and validate risk scores to integrate HRP evaluation into clinical decision-making.

Conclusions

In ACS cases with baseline coronary CT, HRP positive plaques that are non-obstructive outnumber those that are obstructive, even though HRP is more prevalent among obstructive lesions. Non-obstructive HRP confers risk of a magnitude that is clinically comparable to an obstructive HRP negative lesion. HRP should be clinically reported even in the presence of non-obstructive CAD. Future studies should assess methods to integrate HRP and non-obstructive CAD into risk assessment for clinical decision-making.

Funding

This work was supported by the NIH (HL115150) and the Leading Foreign Research Institute Recruitment Program of the National

Research Foundation of Korea, Ministry of Science, ICT & Future Planning (Seoul, Korea).

Conflict of interest: J.K.M. receives funding from the Dalio Foundation, National Institutes of Health, and GE Healthcare. J.K.M. serves on the scientific advisory board of Arineta and GE Healthcare and has an equity interest in Cleerly. B.J.W.C. holds the Saul and Edna Goldfarb Chair in Cardiac Imaging Research, receives support from CV Diagnostix and Auscultations, receives educational support from TeraRecon Inc., and has equity interest in General Electric. H.S. serves on the scientific advisory board of Philips, has equity interest in Covanos Inc., and has a research grant from Medtronic, Abbott Vascular, and Philips. All other authors declared no conflict of interest.

References

- Ambrose JA, Tannenbaum MA, Alexopoulos D, Hjerdahl-Monsen CE, Leavy J, Weiss M *et al.* Angiographic progression of coronary artery disease and the development of myocardial infarction. *J Am Coll Cardiol* 1988;**12**:56–62.
- Chang H-J, Lin FY, Lee S-E, Andreini D, Bax J, Cademartiri F *et al.* Coronary atherosclerotic precursors of acute coronary syndromes. *J Am Coll Cardiol* 2018;**71**: 2511–22.
- Maddox TM, Stanislawski MA, Grunwald GK, Bradley SM, Ho PM, Tsai TT *et al.* Nonobstructive coronary artery disease and risk of myocardial infarction. *JAMA* 2014;**312**:1754–63.
- Lin FY, Shaw LJ, Dunning AM, Labounty TM, Choi JH, Weinsaft JW *et al.* Mortality risk in symptomatic patients with nonobstructive coronary artery disease: a prospective 2-center study of 2,583 patients undergoing 64-detector row coronary computed tomographic angiography. *J Am Coll Cardiol* 2011;**58**: 510–9.
- Hoffmann U, Ferencik M, Udelson JE, Picard MH, Truong QA, Patel MR *et al.* Prognostic value of noninvasive cardiovascular testing in patients with stable chest pain: insights from the PROMISE Trial (Prospective Multicenter Imaging Study for Evaluation of Chest Pain). *Circulation* 2017;**135**:2320–32.
- Adamson PD, Hunter A, Williams MC, Shah ASV, McAllister DA, Pawade TA *et al.* Diagnostic and prognostic benefits of computed tomography coronary

- angiography using the 2016 National Institute for Health and Care Excellence guidance within a randomised trial. *Heart* 2018;**104**:207–14.
7. Virmani R, Kolodgie FD, Burke AP, Farb A, Schwartz SM. Lessons from sudden coronary death. *Arterioscler Thromb Vasc Biol* 2000;**20**:1262–75.
 8. Motoyama S, Sarai M, Harigaya H, Anno H, Inoue K, Hara T et al. Computed tomographic angiography characteristics of atherosclerotic plaques subsequently resulting in acute coronary syndrome. *J Am Coll Cardiol* 2009;**54**:49–57.
 9. Puchner SB, Liu T, Mayrhofer T, Truong QA, Lee H, Fleg JL et al. High-risk plaque detected on coronary CT angiography predicts acute coronary syndromes independent of significant stenosis in acute chest pain: results from the ROMICAT-II trial. *J Am Coll Cardiol* 2014;**64**:684–92.
 10. Ferencik M, Mayrhofer T, Bittner DO, Emami H, Puchner SB, Lu MT et al. Use of high-risk coronary atherosclerotic plaque detection for risk stratification of patients with stable chest pain: a secondary analysis of the promise randomized clinical trial. *JAMA Cardiol* 2018;**3**:144–52.
 11. Tian J, Dauerman H, Toma C, Samady H, Itoh T, Kuramitsu S et al. Prevalence and characteristics of TCFA and degree of coronary artery stenosis: an OCT, IVUS, and angiographic study. *J Am Coll Cardiol* 2014;**64**:672–80.
 12. Motoyama S, Ito H, Sarai M, Kondo T, Kawai H, Nagahara Y et al. Plaque characterization by coronary computed tomography angiography and the likelihood of acute coronary events in mid-term follow-up. *J Am Coll Cardiol* 2015;**66**:337–46.
 13. SCOT-HEART Investigators. Coronary CT angiography and 5-year risk of myocardial infarction. *N Engl J Med* 2018;**379**:924–33.
 14. Mendis S, Thygesen K, Kuulasmaa K, Giampaoli S, Mähönen M, Ngu Blackett K et al.; Writing group on behalf of the participating experts of the WHO consultation for revision of WHO definition of myocardial infarction. World Health Organization definition of myocardial infarction: 2008–09 revision. *Int J Epidemiol* 2011;**40**:139–46.
 15. Thygesen K, Alpert JS, Jaffe AS, Simoons ML, Chaitman BR, White HD et al. Third universal definition of myocardial infarction. *J Am Coll Cardiol* 2012;**60**:1581–98.
 16. Park HB, Lee BK, Shin S, Heo R, Arsanjani R, Kitslaar PH et al. Clinical feasibility of 3D automated coronary atherosclerotic plaque quantification algorithm on coronary computed tomography angiography: comparison with intravascular ultrasound. *Eur Radiol* 2015;**25**:3073–83.
 17. Achenbach S, Giesler T, Ropers D, Ulzheimer S, Derlien H, Schulte C et al. Detection of coronary artery stenoses by contrast-enhanced, retrospectively electrocardiographically-gated, multislice spiral computed tomography. *Circulation* 2001;**103**:2535–8.
 18. Hoffmann U, Moselewski F, Cury RC, Ferencik M, Jang I-K, Diaz LJ et al. Predictive value of 16-slice multidetector spiral computed tomography to detect significant obstructive coronary artery disease in patients at high risk for coronary artery disease. *Circulation* 2004;**110**:2638–43.
 19. Maurovich-Horvat P, Schlett CL, Alkadhi H, Nakano M, Otsuka F, Stolzmann P et al. The napkin-ring sign indicates advanced atherosclerotic lesions in coronary CT angiography. *JACC Cardiovasc Imaging* 2012;**5**:1243–52.
 20. Williams MC, Moss AJ, Dweck M, Adamson PD, Alam S, Hunter A et al. Coronary artery plaque characteristics associated with adverse outcomes in the SCOT-HEART study. *J Am Coll Cardiol* 2019;**73**:291–301.
 21. Mauriello A, Servadei F, Zoccai GB, Giacobbi E, Anemona L, Bonanno E et al. Coronary calcification identifies the vulnerable patient rather than the vulnerable plaque. *Atherosclerosis* 2013;**229**:124–9.
 22. Stone GW, Maehara A, Lansky AJ, de Bruyne B, Cristea E, Mintz GS et al. A prospective natural-history study of coronary atherosclerosis. *N Engl J Med* 2011;**364**:226–35.
 23. Cury RC, Abbara S, Achenbach S, Agatston A, Berman DS, Budoff MJ, et al. CAD-RADS™: coronary artery disease—reporting and data system: an expert consensus document of the Society of Cardiovascular Computed Tomography (SCCT), the American College of Radiology (ACR) and the North American Society for Cardiovascular Imaging (NASCI). Endorsed by the American College of Cardiology. *J Am Coll Radiol* 2016;**13**:1458–66.e9.
 24. Adamson PD, Williams MC, Dweck MR, Mills NL, Boon NA, Daghm M et al. Guiding therapy by coronary CT angiography improves outcomes in patients with stable chest pain. *J Am Coll Cardiol* 2019;**74**:2058–70.
 25. Bittner DO, Mayrhofer T, Puchner SB, Lu MT, Maurovich-Horvat P, Ghemigian K et al. Coronary computed tomography angiography-specific definitions of high-risk plaque features improve detection of acute coronary syndrome. *Circ Cardiovasc Imaging* 2018;**11**:e007657.
 26. Lee S-E, Chang H-J, Rizvi A, Hadamitzky M, Kim Y-J, Conte E et al. Rationale and design of the Progression of Atherosclerotic Plaque Determined by Computed Tomographic Angiography IMaging (PARADIGM) registry: a comprehensive exploration of plaque progression and its impact on clinical outcomes from a multi-center serial coronary computed tomographic angiography study. *Am Heart J* 2016;**182**:72–9.